

## Some advantages of intermediate band solar cells based on type II quantum dots

Antonio Luque, Pablo G. Linares, Alex Mellor, Viacheslav Andreev, and Antonio Marti

Citation: *Appl. Phys. Lett.* **103**, 123901 (2013); doi: 10.1063/1.4821580

View online: <http://dx.doi.org/10.1063/1.4821580>

View Table of Contents: <http://apl.aip.org/resource/1/APPLAB/v103/i12>

Published by the [AIP Publishing LLC](#).

---

### Additional information on *Appl. Phys. Lett.*

Journal Homepage: <http://apl.aip.org/>

Journal Information: [http://apl.aip.org/about/about\\_the\\_journal](http://apl.aip.org/about/about_the_journal)

Top downloads: [http://apl.aip.org/features/most\\_downloaded](http://apl.aip.org/features/most_downloaded)

Information for Authors: <http://apl.aip.org/authors>



**PulseLine™ Ultrafast Laser Optics**

The PulseLine family includes a number of standard, in-stock products which are ready to ship, and fully customized optics for volume applications

**PULSELINE PRODUCTS**

- MIRRORS
- BEAMSPLITTERS
- POLARIZING OPTICS (PLATES AND CUBES)
- PRISMS
- ANTI-REFLECTION WINDOWS

**CVI Laser Optics**  
cvilaseroptics@idexcorp.com  
cvilaseroptics.com

**IDEX**  
OPTICS & PHOTONICS

ATFilms | Precision Photonics | CVI Laser Optics | Melles Griot | Semrock

## Some advantages of intermediate band solar cells based on type II quantum dots

Antonio Luque,<sup>1,2,a)</sup> Pablo G. Linares,<sup>2</sup> Alex Mellor,<sup>2</sup> Viacheslav Andreev,<sup>1</sup> and Antonio Martí<sup>2</sup>

<sup>1</sup>*Ioffe Physico-Technical Institute, 26 Polytekhnicheskaya, St.Petersburg 194021, Russia*

<sup>2</sup>*Universidad Politécnica de Madrid, Instituto de Energía Solar, 28040 Madrid, Spain*

(Received 10 July 2013; accepted 1 September 2013; published online 17 September 2013)

Unlike Type I, Type II quantum dots do not have hole bound states. This precludes that they invade the host semiconductor bandgap and prevents the reduction of voltage in intermediate band solar cells. It is proven here that the optical transition between the hole extended states and the intermediate bound states within the host bandgap is much stronger than in Type I quantum dots, increasing the current and making this structure attractive for manufacturing these cells. © 2013 AIP Publishing LLC. [<http://dx.doi.org/10.1063/1.4821580>]

The intermediate band solar cell was proposed to increase the efficiency of solar cells.<sup>1</sup> An intermediate band (IB) is formed within the bandgap of a semiconductor that acts as a stepping-stone to transfer an electron from the valence band (VB) to the conduction band (CB) via the absorption of two sub-bandgap photons. In this way, the photocurrent is increased. The voltage is, in principle, not reduced because the IB material is sandwiched between two ordinary semiconductors (p- and n-type), so that the IB is not in contact with the metallic electrodes of the solar cell, which are deposited on the front and back surfaces. In the case of quantum dot (QD) IB solar cells, the IB is formed by the energy levels of bound states, caused by the QDs detached from the CB and located within the bandgap of the host (or barrier) semiconductor.

Practical QD IB solar cells have not, as of yet, been produced. The main reason is the weak photon absorption of the QDs that have been used but also an undesired voltage reduction due to these QDs. The purpose of this paper is to examine other QD configurations, looking for ones with stronger absorption and that reduce the voltage decrease.

Most QD IB solar cells are made of InAs QDs in a host GaAs semiconductor. They are Type I QDs, whose bandgap is a shrunken form of the host bandgap, as shown in Figure 1. In this QD, a set of bound states is formed at energy levels within the host material bandgap, appearing to be near both the CB and VB. The latter are prolific and closely spaced, due to the large effective mass of the heavy holes. The states corresponding to the light holes, which are much fewer in number, are also intercalated. Some bound states also appear within the corresponding host material band (shown in Figure 1 for holes but also occurring with electrons) and are called virtual bound states. The energy spectrum caused by the QDs can be calculated under the box shaped QD hypothesis by solving the effective mass equations for each band,<sup>2</sup> using the separation-of-variables method.<sup>3</sup> The quantum numbers used for labeling the states refer to the one-dimensional solutions for each coordinate. The quantum

numbers may be preceded with CB, IB, HH (heavy holes), or LH (light holes) to distinguish the band.

It must be taken into consideration that, due to the negative effective mass of the holes, the pedestal appearing in the VB, due to the Type I QD, acts similarly to the well in the CB and has the potential of forming hole bound states in the VB.

For sub-bandgap photons, optical absorption is produced between the heavy and light hole BSs and the IB BSs. This has been studied in the context of IB solar cells.<sup>2</sup> Absorptions between the IB states and the host material CB virtual bound states are also produced to allow operation of the IB solar cells. In addition to the transitions between bound states, photon absorption also occurs from transitions between extended states and bound states (or between bound states and extended states).

In Type I QDs, there are important sub-bandgap absorptions between hole bound states that have invaded the bandgap, shown in Figure 1, and some virtual bound states in the CB. In practice, this is a reduction of the bandgap caused by the QDs that facilitates the recombination and is an important factor in the observed voltage reduction of the IB solar cells.<sup>4</sup> These hole bound states do not exist in Type II QDs, where the bandgaps for the QD and the host material are staggered, and therefore they are expected to present much less voltage reduction.

For vertical (*z*-directed), non-polarized illumination, the transitions are proportional to  $(|\langle \mathcal{E} | x | \mathcal{E}' \rangle|^2 + |\langle \mathcal{E} | y | \mathcal{E}' \rangle|^2)/2$ , where  $|\mathcal{E}\rangle$  and  $|\mathcal{E}'\rangle$  are the initial and final electronic state of the transition and all states are assumed to be normalized. Since the matrix elements represent integrals, a necessary condition for strong absorption is the strong superposition of the initial and final states. However, the superposition integral between an extended state and a bound state is very weak because of the low superposition. In fact, the normalization of the extended states leads to a negligible value of their amplitude at any given point and thus, at the points where the bound state amplitude is large. However, the observed photon absorption is equal to the sum of the absorptions of each transition between couples of states. In the case of extended states, they form a continuum of energies. The observed absorption, therefore, is the product of a

<sup>a)</sup>Author to whom correspondence should be addressed. Electronic mail: [luque@ies-def.upm.es](mailto:luque@ies-def.upm.es). Telephone: +(34) 609 461413. Fax: +(34) 915446341.

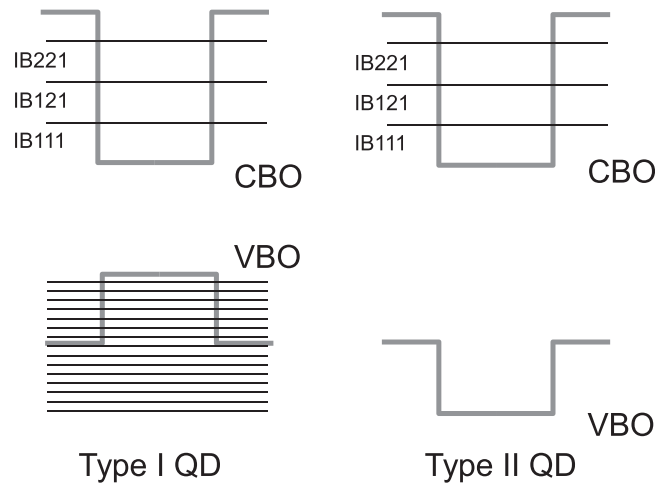


FIG. 1. Schematic of Type I and Type II quantum dots showing some of the energy levels for bound states and the conduction band (CBO) and valence band (VBO) offsets, respectively.

negligible transition times the number of concurrent transitions, so that the strength of the observed absorption is undetermined. This indetermination has been removed<sup>5</sup> for the InAs/GaAs system. It shows that the absorption for transitions between bound states, and extended states are much weaker than the absorption between couples of bound states.

Using the effective mass Schrödinger equation for holes (the same as the one for electrons with changed signs), the well appearing in the Type II QD VB is to be treated as a pedestal for ordinary electrons. It is a textbook exercise to show that pedestals do not sustain bound states. The only wavefunctions are the extended states with energy above the pedestal base (for holes, below the VB top of the host material). For energy below the pedestal top, the electron cannot easily penetrate the pedestal. This wavefunction is hyperbolic, with a minimum in the center of the pedestal. Outside, it is harmonic, as extended functions usually are. For energy above the pedestal top, the wavefunctions are harmonic everywhere but, using a classical analogue, their kinetic energy (and therefore the speed) is reduced when they pass over the pedestal, so that there is an increased probability of finding the electron inside the pedestal. This is the opposite of the performance of a well. Over the well, the electron speed increases and the probability per unit of volume of finding the electron over the well is reduced. Figure 2 presents a simple one-dimensional calculation, showing the increased amplitude of the wavefunction for Type II QDs. Resonances are characteristic of the quantum behavior and may lead to strong amplitude at certain energies.

Since bound states in the IB are bound around the QD, the overlap integral of the photon absorption element of the matrix is larger for extended states in Type II than in Type I QDs. The trade-off, then, between a small overlap and a high number of states may now benefit the extended states.

To this end, we compare the InAs/GaAs cell labeled SB in Ref. 6 with an unreal Type II structure, having the same parameters as those of the InAs/GaAs referred system, but with the pedestal in the VB (acting as a well for holes) transformed into a well (acting as a pedestal for holes). The absorption coefficients for transitions between extended

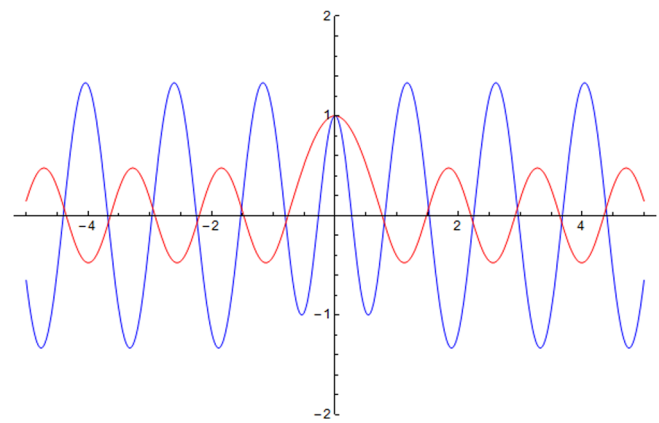


FIG. 2. One-dimensional, non-normalized extended wavefunctions: Red for a pedestal of 0.21 eV and blue (with higher amplitude) for a well of the same depth. In both cases  $ka = 3.5$  corresponding to a kinetic energy of 0.27 eV. The effective mass is 0.027 times the electron mass in the vacuum. The abscissas are normalized to the QD half length (the QD extends from  $-1$  to  $+1$ ).

states in the VB and bound states in the IB have been calculated for the system indicated.<sup>5</sup>

Most of this work can be specifically applied to this case. Only the one-dimensional solutions for the effective mass equation have to be recalculated for the case of a pedestal. The three-dimensional extended state is exactly the product of the three one-dimensional solutions<sup>3</sup> (separation of variables holds exactly in this case). To calculate the elements of the optical transition matrix, we have used the Empiric  $k \cdot p$  Hamiltonian<sup>2</sup> and, once the elements of the matrix are calculated, they are introduced in the absorption formula and integrated in three dimensions for all the values of the extended-function wavevectors.<sup>6</sup> As has been said, our QDs are modeled as boxes (parallelepipeds) and symmetry considerations are used to reduce the number of calculations.<sup>7</sup> Figure 3 shows the absorption for the Type II unreal case as compared to the all-bound and all-extended absorption curves ending in all of the IB states for the real InAs/GaAs case. As expected, the absorption in transitions from the VB extended states to the IB bound states is several hundred times stronger in Type II QDs than in Type I. However, they are still about ten times smaller than the transitions

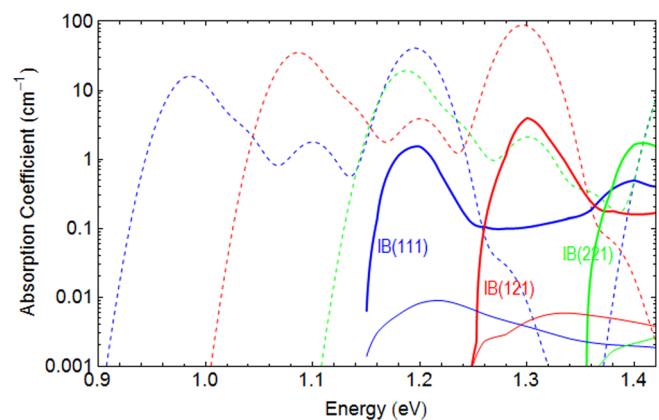


FIG. 3. Absorption coefficient from VB states to IB states indicated by the colored labels. Thick curves are for the Type II QD extended states, thin continuous lines are for the Type I QD extended states and dashed lines are for Type I bound states. In the IB(121)/211) degenerate state the label refers to one of the states but the curve includes both.

between bound states of Type I QDs. Note that the absorption for the extended states starts at the position of the IB bound state energy level measured from the top of the VB, which, when the comparison exercise is done, is the same for type I and type II QDs. The transitions from the VB bound states start at a lower energy level, because the energy positions of the hole bound states invade the bandgap. The two peaks in each curve correspond to the onset of the absorption from the heavy holes (of less photon energy) and light holes. Data are from this paper (for the Type II QDs) and from Refs. 5 and 7 for the extended and the bound states of the type I QD, respectively.

The application of Type II QDs in solar cells is an object of high interest. In many cases, it refers to colloidal QDs for organic semiconductors, with application to solar cells.<sup>8</sup> Adding antimony to the QD in a III-V host semiconductor a Type II band alignment is produced in the CB (not in the VB as in Figure 1) and this has been proven to enhance effectively the infrared photocurrent increase;<sup>9</sup> however, the voltage is strongly reduced. We think such structure produces the bandgap shrinkage already discussed as being characteristic of Type I QDs, but no IB at all. Adding antimony to the III-V host material and keeping the InAs for the QDs produces the desired VB Type II alignment as shown in Figure 1. The GaAsSb as host material for QDs has been profusely investigated since, at least, 2003 (Ref. 10) and recent work<sup>11</sup> reports enhanced infrared photocurrent and, simultaneously, increased open circuit voltage, as intended in this paper although the addition of Sb to the GaAs reduces the bandgap and consequently the open circuit voltage.

In this paper, we calculate the case of InAs QDs in a host semiconductor with antimony producing a Type II band alignment in the VB. The bandgap, offsets CBO and VBO and effective masses of electrons and of heavy and light holes in the QD and in the barrier material have been calculated using Ref. 12. To increase the bandgap, we add Al to the host material. Much less previous work is available based on such quaternaries.<sup>13</sup> There are a very large number of them formed with Al, Ga, As, and Sb. We have restricted our search to those lattice-matched with InP, which is a materials grown in bulk crystals and may be used as a substrate for the formation of a lattice-matched quaternary. Taking into account, the energy spectrum appearing in Figure 4 we have chosen  $\text{Al}_{0.64}\text{Ga}_{0.36}\text{As}_{0.54}\text{Sb}_{0.46}$  as a host material for InAs QDs because their levels are reasonably well situated to cover a wide sub-bandgap range of absorption while avoiding overlap between the  $\text{VB} \rightarrow \text{IB}$  and the  $\text{IB} \rightarrow \text{CB}$  transitions, the latter not studied here because they are usually not limiting (and they are easily studied in the frame of a single effective mass equation). The parameters of this system are presented in Table I. The energy spectrum was obtained by the separation-of-variables method, but the energies are accurate for the IB states and reasonably accurate for the virtual bound states. Note that there are five levels in the IB: (1,1,1), (1,2,1)/(2,1,1) (both degenerate), (2,2,1), (1,1,2), and (1,3,1)/(3,1,3). The last two levels were absent in the InAs/GaAs case previously studied. As matter of fact, the number of states depends on the CB offset, on the effective mass used (actually, the one for the QD) and the QD size. The dependence on size is very strong. To have only five BS levels

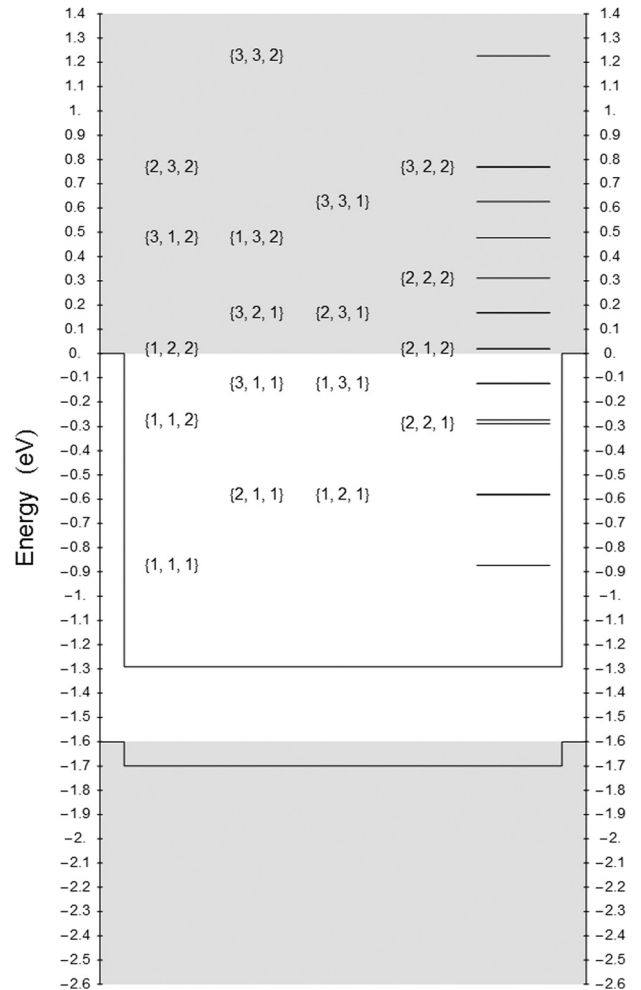


FIG. 4. Energy levels for the IB bound states (within the bandgap) and the virtual bound states (in the grey region) of an InAs QD in a  $\text{Al}_{0.64}\text{Ga}_{0.36}\text{As}_{0.54}\text{Sb}_{0.46}$  host. Grey regions sustain a continuous of extended eigenfunctions.

(so facilitating the calculations), we have reduced the QD base from 16 nm in the InAs/GaAs case to 10 nm in the current case.

Figure 5 shows the absorptions calculated in this case. No bound state exists for the VB. The absorption is quite strong and is not very different than the one obtained for bound states in the InAs/GaAs case. Neither the InAs/GaAs

TABLE I. Parameter calculations for the InAs QDs in  $\text{Al}_{0.64}\text{Ga}_{0.36}\text{As}_{0.54}\text{Sb}_{0.46}$ .

Parameter	Units	Value
$\text{Al}_{0.64}\text{Ga}_{0.36}\text{As}_{0.54}\text{Sb}_{0.46}$ bandgap	eV	1.6016
CB InAs offset	eV	1.2908
VB InAs offset	eV	-0.0976
InAs bandgap (accounting strain)	eV	0.4085
Electron effective mass (in InAs) ratio to free electron mass		0.0255
Heavy hole effective mass (in InAs) ratio to free electron mass		0.333
Light hole effective mass (in InAs) ratio to free electron mass		0.027
QD base side	nm	10
QD height	nm	6

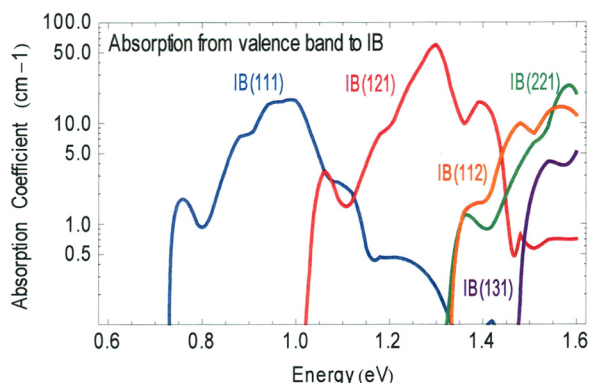


FIG. 5. Absorption coefficient from VB extended states to IB states of an InAs QD in a  $\text{Al}_{0.64}\text{Ga}_{0.36}\text{As}_{0.54}\text{Sb}_{0.46}$  host. The labels indicate the final states. For degenerate states, only one is expressed, but the curve refers to both added.

nor the InAs/  $\text{Al}_{0.64}\text{Ga}_{0.36}\text{As}_{0.54}\text{Sb}_{0.46}$  are optimized material systems.

In summary, we expect it will possible to find a Type II QD material with absorption strength, based on extended state  $\rightarrow$  bound state transitions, similar or better than that in Type I QD materials, which is based on bound state  $\rightarrow$  bound state transitions. Furthermore, we have already stressed the absence of the bandgap reduction due to the penetration of the HH bound states into the host material bandgap in Type I QDs, leading to an undesirable voltage reduction. These expectations, theoretically explained by our model, seem to have already been experimentally confirmed.<sup>11</sup> Therefore, Type II QDs, with no confining potential in the VB, are recommended for further experimental research in quest of an increased sub-bandgap current with less voltage reduction. With these modifications, it is

possible to envisage IB solar cells that exceed the efficiency of solar cells made in the host material without QDs, in particular if the density of QDs is increased.<sup>14</sup>

The authors want to acknowledge that this work has been supported by the Mega-grant No. 14B25.31.0020 from the Russian Ministry of Education and Science, the EC NGCPV (283798) grant and the NUMANCIA II (ESE2009-ENE1497) grant from the Madrid Regional Government. They also want to acknowledge helpful comments by an anonymous referee.

- <sup>1</sup>A. Luque and A. Martí, *Phys. Rev. Lett.* **78**, 5014–5017 (1997).
- <sup>2</sup>A. Luque, A. Martí, E. Antolín, P. G. Linares, I. Tobías, I. Ramiro, and E. Hernández, *Sol. Energy Mater. Sol. Cells* **95**, 2095–2101 (2011).
- <sup>3</sup>A. Luque, A. Mellor, I. Tobías, E. Antolín, P. G. Linares, I. Ramiro, and A. Martí, *Physica B* **413**, 73–81 (2013).
- <sup>4</sup>A. Luque, A. Martí, and C. Stanley, *Nature Photon.* **6**, 146–152 (2012).
- <sup>5</sup>A. Luque, A. Mellor, I. Ramiro, E. Antolín, I. Tobías, and A. Martí, *Sol. Energy Mater. Sol. Cells* **115**, 138–144 (2013).
- <sup>6</sup>E. Antolín, A. Martí, C. D. Farmer, P. G. Linares, E. Hernández, A. M. Sánchez, T. Ben, S. I. Molina, C. R. Stanley, and A. Luque, *J. Appl. Phys.* **108**, 064513 (2010).
- <sup>7</sup>A. Luque, A. Mellor, E. Antolín, P. G. Linares, I. Ramiro, I. Tobías, and A. Martí, *Sol. Energy Mater. Sol. Cells* **103**, 171–183 (2012).
- <sup>8</sup>S. Kim, B. Fisher, H. J. Eisler, and M. Bawendi, *J. Am. Chem. Soc.* **125**, 11466–11467 (2003).
- <sup>9</sup>R. B. Laghumavarapu, A. Moscho, A. Khoshakhlagh, M. El-Emawy, L. F. Lester, and D. L. Huffaker, *Appl. Phys. Lett.* **90**, 173125 (2007).
- <sup>10</sup>K. Akahane, N. Yamamoto, and N. Ohtani, *Physica E* **21**, 295–299 (2004).
- <sup>11</sup>W. S. Liu, H. M. Wu, F. H. Tsao, T. L. Hsu, and J. I. Chyi, *Sol. Energy Mater. Sol. Cells* **105**, 237–241 (2012).
- <sup>12</sup>P. G. Linares, A. Martí, E. Antolín, and A. Luque, *J. Appl. Phys.* **109**, 014313 (2011).
- <sup>13</sup>N. Kuze, H. Goto, M. Matsui, and I. Shibusaki, *J. Vac. Sci. Technol. B* **16**, 2644–2649 (1998).
- <sup>14</sup>J. Tatebayashi, A. Khoshakhlagh, S. H. Huang, L. R. Dawson, G. Balakrishnan, and D. L. Huffaker, *Appl. Phys. Lett.* **89**, 203116 (2006).